

Tracking Dark Excitons with Exciton-Polaritons

D. Schmidt,¹ B. Berger,¹ M. Kahlert,¹ M. Bayer,^{1,2} C. Schneider,³
S. Höfling,³ E. S. Sedov,^{4,5} A. V. Kavokin,^{5,6,7} and M. Aßmann¹

¹*Experimentelle Physik 2, Technische Universität Dortmund, D-44221 Dortmund, Germany*

²*A. F. Ioffe Physical-Technical Institute,*

Russian Academy of Sciences, St Petersburg 194021, Russia

³*Technische Physik, Universität Würzburg, 97074 Würzburg, Germany*

⁴*Vladimir State University named after A. G. and N. G. Stoletovs,
Gorky str. 87, 600000, Vladimir, Russia*

⁵*School of Physics and Astronomy, University of Southampton,
SO17 1NJ Southampton, United Kingdom*

⁶*Spin Optics Laboratory, St. Petersburg State University,
Ulanovskaya 1, Peterhof, St. Petersburg 198504, Russia*

⁷*L.A.S.E.- Laboratory for Advanced Solar Energy,
National University of Science and Technology MISiS,
119049 Leninskiy prosect 6. Moscow, Russia*

(Dated: May 15, 2022)

Abstract

Dark excitons are of fundamental importance for a wide variety of processes in semiconductors, but are difficult to investigate using optical techniques due to their weak interaction with light fields. We reveal and characterize dark excitons injected by non-resonant pulsed excitation in a semiconductor microcavity structure containing InGaAs/GaAs quantum wells by monitoring their interactions with the bright lower polariton mode. We find a surprisingly long dark exciton lifetime of more than 20 ns which is longer than the time delay between two consecutive pulses. This creates a memory effect that we clearly observe through the variation of the time-resolved transmission signal. We propose a rate equation model that provides a quantitative agreement with the experimental data.

A detailed understanding of the nature of electronic excitations in semiconductor crystals is fundamental in order to explain their dynamics, collective interactions and many-body effects. Optical spectroscopy provides a convenient range of characterisation tools for those excitations that are bright, which means that they can absorb or emit light. It is much more complicated to gain experimental access to optically inactive or dark excitations which interact weakly or not at all with light. So called dark excitons are typical representatives of such excitations. Still, their properties are decisive for a wide range of systems ranging from semiconductor monolayers [1] and light harvesting complexes [2] to quantum dots [3–5], where dark excitons form an essential building block for generation of on-demand entangled photon cluster states [6].

Here, we demonstrate that a quasi-resonantly driven polariton condensate is a sensitive probe for the presence of dark excitons and vice versa dark excitons can be utilized to introduce long-lived potentials for a polariton system. Exciton-polaritons are composite quasi-particles resulting from the strong coupling of photons and bright excitons in a microcavity structure containing embedded quantum wells. They are known to exhibit several kinds of bistability [7, 8], most prominently in the transmission curve when probed quasi-resonantly at an energy slightly above the lower polariton branch using a narrow cw laser [9]. We first realize this kind of polariton bistability using the following setup: The sample is a planar GaAs λ cavity consisting of 26 top and 30 bottom GaAs/AlAs distributed Bragg reflector layer pairs, containing six $\text{In}_{0.1}\text{Ga}_{0.9}\text{As}$ quantum wells placed at the central antinodes of the confined light field. The sample shows a Rabi splitting of about 6 meV and is mounted on the ring-shaped cold finger of a continuous flow helium cryostat at a temperature of 14.8 K. The measurements are performed at a positive detuning of 1.8 meV between the cavity and the exciton mode. The linearly polarized cw probe beam is provided by a M-Squared Sol-sTis cw Ti:sapphire laser with a line width below 100 kHz. The laser beam is focused to a spot diameter of about 40 μm onto the sample at normal incidence at a detuning of 650 μeV with respect to the empty cavity lower polariton mode, which shows a line width of about 170 μeV . The light transmitted through the cavity is detected using a 400 MHz bandwidth photodiode.

Figure 1(a) demonstrates the measured hysteresis cycle of the transmission through the sample showing stable off- and on-states and a bistable region in between, which is a consequence of the repulsive interaction of polaritons with the same spin [10]. Accordingly, the

lower polariton mode experiences a spectral blueshift that depends on the polariton occupation number. Thus, it is the spectral overlap between the lower polariton mode and the probe beam that governs the transmission of the latter through the cavity. The presence of other carriers will also introduce a shift of the polariton mode [11–13]. As this shift directly translates to a modified probe beam transmission, the latter becomes a sensitive tool to detect the presence of other carriers and measure the strength of their interactions.

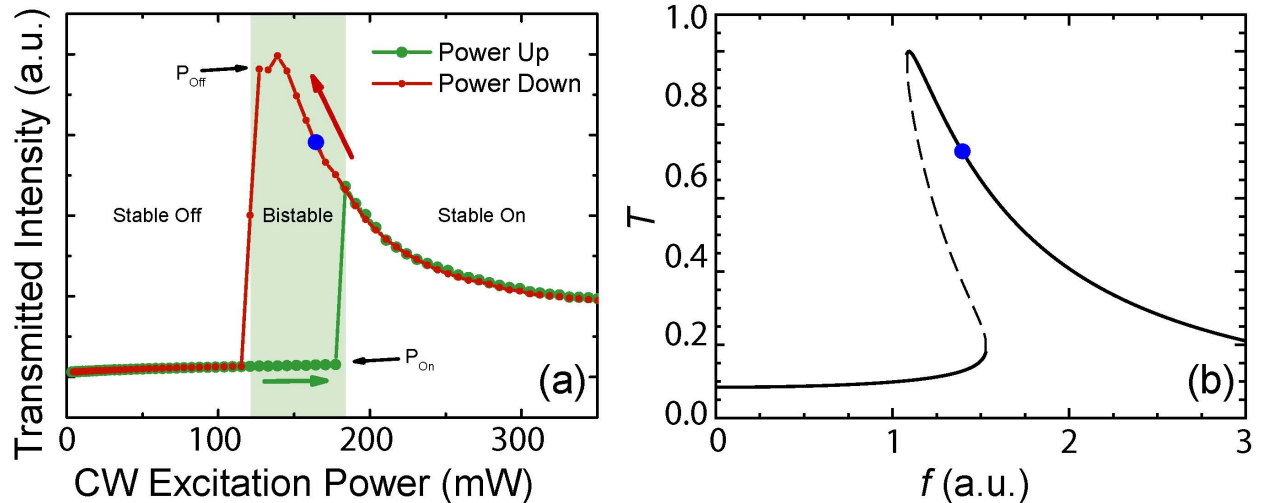


FIG. 1. (a) Measured transmission intensity through the sample as a function of the cw excitation pump power. (b) Transmission through the structure simulated using Eqs. (1)–(2). Blue circles denotes the working position for further discussion.

Next, we introduce additional carriers into the system and monitor their dynamics using the setup just presented. To this end, we employ a pulsed Ti:Sapphire laser with a pulse repetition rate of 75.39 MHz and a pulse duration of about 100 fs to perform far off-resonant excitation at the center of the fourth Bragg minimum of the microcavity structure at 737 nm. The off-resonant pump is focused to the same sample position as the probe laser, but has a larger diameter of $75 \mu\text{m}$ to ensure that the probe laser samples only the central region of the pump spot. It should be noted that the sample does not show spontaneous condensation under non-resonant excitation. A transition into the weak coupling regime will occur at some point, but all pump powers used here are still below the threshold density for this transition [14].

In order to investigate time scales longer than the temporal distance between two pulses, we use an electro-optical modulator to gate the non-resonant pump beam. The gate operates

at a repetition rate of 100 kHz and opens for 90 or 103 ns, which creates pulse trains of seven or eight full consecutive pulses. We set the intensity of the probe laser to an intensity in the middle of the upper branch of the bistability curve as indicated by the blue dot in Fig. 1(a) and record the time-resolved change of its relative transmission with respect to the non-resonant pump pulses. Figure 2 shows a typical trace of the relative transmission. Shortly after a pulse arrives on the sample, the probe transmission diminishes significantly and slowly increases again afterwards. Surprisingly, we find that the relative transmission does not fully recover until the next pulse arrives. Instead the suppression builds up quickly over the course of the first four pulses. Afterwards the peak suppression continues to increase slowly with every additional pulse. After the last pulse of the train has arrived on the sample, the transmission slowly recovers back to the initial value on a long timescale of tens of ns.

As the reduced transmission translates to a spectral shift of the lower polariton mode, these results raise questions about the nature of the carriers causing this shift. While there have been numerous studies on the dynamics of polariton condensates after non-resonant excitation, the focus has so far been on bright excitations. Free carriers may relax and form bright exciton-like polaritons at large wavevector, which in turn relax down the polariton dispersion via spontaneous or stimulated scattering until they reach the ground state and join the condensate. Both the changes in population dynamics and the presence of free carriers will result in changes of the relative transmission, but they will do so on the short timescale required for carriers to form polaritons, reach the ground state and leave the cavity. Both are typically on the order of tens of ps [15]. Even considering a possible slow-down of relaxation at small carrier densities, an upper limit for this timescale is given by the bright exciton lifetime. For high-quality quantum wells, it may be as short as tens of ps, but even for low-quality structures, it will usually not exceed the bulk value of about 1 ns [16]. Therefore, bright carriers fail to explain the long timescale seen in the experiment. This suggests that optically dark excitations play a significant role for long times after non-resonant excitation.

In order to validate this assumption, we modelled the kinetics of the system by solving the Gross-Pitaevskii equations for the bright polariton condensate wave function Ψ coupled to the rate equations for the occupation number of an incoherent reservoir of optically inactive

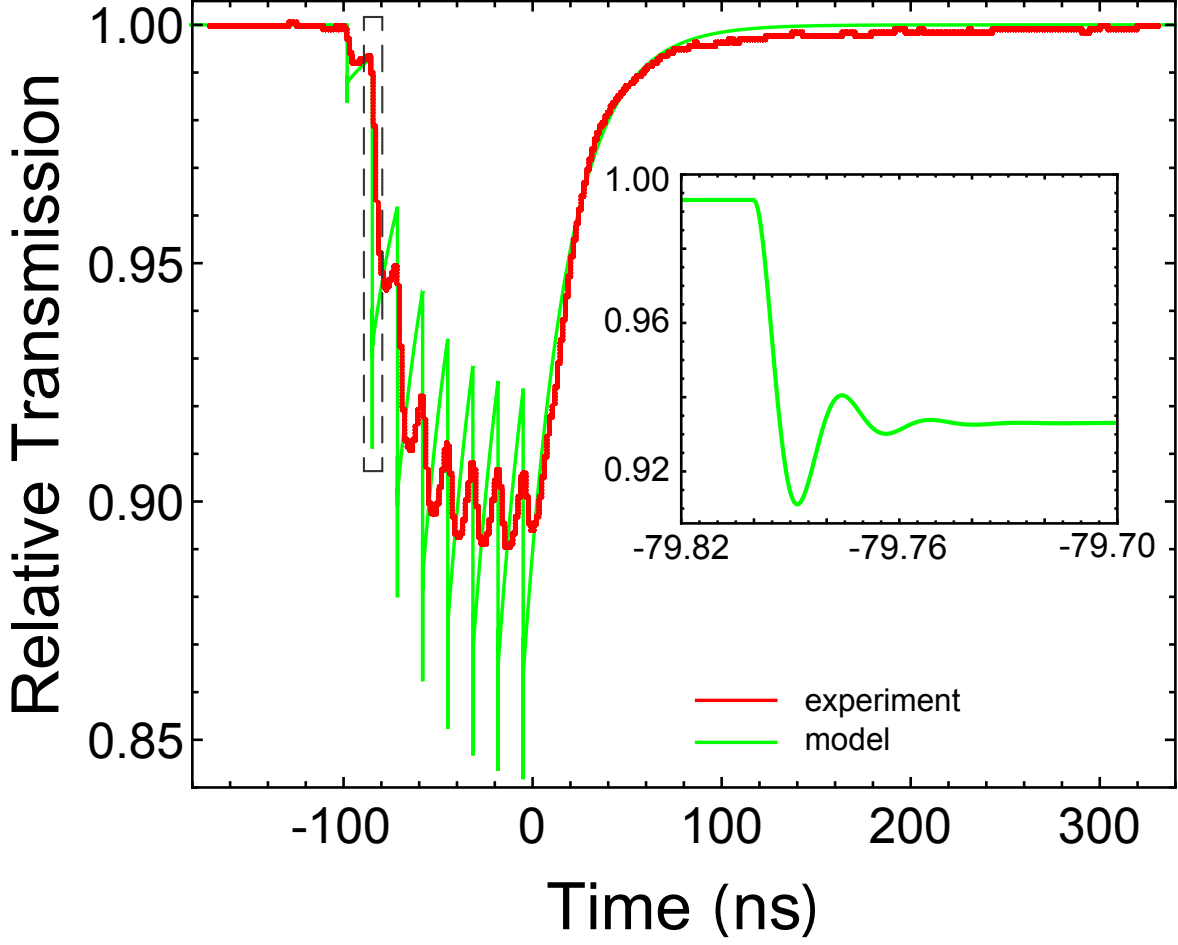


FIG. 2. Relative transmission intensity resolved in time. The gate consists of $n = 7$ pulses. Red and green curves correspond to the experiment and model, respectively. The slow component shows an exponential decay on a timescale of 22 ns, while the inset shows fast polariton dynamics on the picosecond scale corresponding to the schematic dashed frame in the main figure. The cw pump power corresponds to blue dots in Fig. 1. The additional small peak at the beginning of the gate is an artifact due to non-instantaneous opening of the gate.

excitons N_X :

$$i\hbar d_t \Psi = [\delta_p + V_b(t) - i\hbar\gamma_C/2] \Psi + if, \quad (1)$$

$$d_t N_X = P(t) - \gamma_X N_X. \quad (2)$$

In (1) δ_p is responsible for the detuning of the resonant pump energy from the the bare lower polariton energy, which we choose as a reference. $V_b(t) = g_C|\Psi|^2 + g_R N_X$ describes the blueshift of the polariton energy due to the intra-condensate polariton interactions and

the interaction with the reservoir excitons; g_C and g_X are the corresponding interaction constants. γ_C is the polariton relaxation rate, f is the amplitude of the resonant cw pump. Equation (2) is the rate equation for inactive dark reservoir excitons pumped incoherently by the modulated in time optical pump $P(t)$. The exciton reservoir relaxes at a rate of γ_X .

Under solely resonant pumping, when one assumes $P = 0$, the system has been extensively considered for bistability and related effects. [9, 17, 18]. Following [18], within the one-mode approximation, $\Psi = \psi_p e^{-iE_p t/\hbar}$, for the driven polariton mode ψ_p we obtain:

$$|\psi_p|^2 = \frac{F}{(\delta_p + g_C |\psi_p|^2)^2 + (\hbar\gamma_C/2)^2}, \quad (3)$$

where $F = f^2$ describes the resonant pump intensity. $N = |\psi_p|^2$ is the occupation number of the driven polariton mode. The transmission intensity through the structure which is in the focus of our consideration in this Letter now can be estimated as $T \propto N/F$. Figure 1(b) shows the transmission T as a function of the cw resonant pump amplitude f . Two branches (solid) corresponding to stable solutions of Eq. (3) nicely qualitatively reproduce the experimental dependence for the transmission shown in Fig. 1(a). The parameters used for modelling are given in Ref. [19].

To model the transmission dynamics, we solve Eqs. (1)–(2) numerically in the presence of the non-resonant optical gate. We take the latter as a train of sub-picosecond Gaussian pulses in the form $P(t) = \sum_{j=0}^{n-1} P_0 \exp[-(t - j/\nu - t_0)^2/w^2]$, where n is the number of pulses in one train, ν is the pulse repetition rate in one train, t_0 is the time of arrival of the first pulse peak, w is a single pulse duration. The green curve in Fig. 2 shows the transmission variation in time in presence of the optical gate of $n = 7$ pulses. To take into account non-instantaneous opening of the gate, we assume an additional pulse enters the system prior to the main train, and possessing energy of one tenth of subsequent pulses. The simulated slow dynamics at the nanosecond scale fully reproduces the measurements. The inset in Fig. 2 shows fast dynamics on the scale of tens of picoseconds. It reflects the population relaxation after the pulse arrival. The monotonic region after arrival of the last pulse in Fig. 2 allows us to estimate the lifetime of dark excitons as $1/\gamma_X \approx 22$ ns, see Supplementary material [14] for the details of the estimation.

Several types of excitations could be at the heart of the long-lived line shifts. Parity-forbidden and spatially indirect excitons are unlikely candidates. In addition, coherent multidimensional spectroscopy has demonstrated that they usually show some weak coupling

to bright states, which limits their lifetime drastically [20]. For biexcitons, also much shorter lifetimes are expected [12]. Two kinds of dark excitations should be retained as candidates for the observed dark carrier population. First, spin-forbidden dark excitons with an exciton spin projection of $J_z = \pm 2$ may form under non-resonant excitation. These excitations can only decay non-radiatively or by spin relaxation towards a bright state. Second, spin-allowed carriers with $J_z = \pm 1$ may form at large wavevectors k_{\parallel} . If their wavevector exceeds that of light inside the medium, they also cannot couple to light fields and are thus optically dark. A closer look at the typical relaxation processes already sheds some light on the processes taking place.

In quantum wells not embedded inside a microcavity, the spin relaxation time between dark $J_z = \pm 2$ excitons and bright $J_z = \pm 1$ excitons is governed by the short range exchange interaction between excitons [21], which causes an energy splitting of about $80 \mu\text{eV}$ between the bright and dark states with dark states being at lower energy [22]. This splitting results in a spin relaxation timescale of about 80 ps. For quantum wells embedded into a microcavity, the situation changes drastically. In the strong coupling regime, the light-matter interaction shifts the bright state to lower energies by a value given by half the Rabi energy. As this splitting is significantly larger than the splitting in bare quantum wells, also the spin relaxation time by exciton-exciton interaction is expected to become much longer. However, as the splitting depends on k_{\parallel} and due to symmetry reasons, mixing of bright and dark states occurs at $k_{\parallel} \neq 0$ [23], especially in the bottleneck region [24], it is expected that primarily dark excitons with $J_z = \pm 2$ at $k_{\parallel} = 0$ will show a drastically enhanced lifetime. Due to the large value of the Rabi splitting, it is expected that relaxation will mostly occur via phonons to bright polariton states in the bottleneck region of the dispersion and it will therefore not depend strongly on the dark exciton density. For $J_z = \pm 1$ excitons at large wavevector, momentum and energy relaxation towards the optically active region is supposed to be the most important relaxation channel. Thus, exciton-exciton scattering should play a significant role and some kind of density dependence is expected.

In order to gain some insight on these scenarios and also to estimate the magnitude of suppression of transmission we are able to achieve, we compared the dynamics of the suppression for different non-resonant pump powers as shown in figure 3. First, indeed the suppression can be enhanced by pumping more strongly. The transmission can be reduced to values below 15% of its initial value. Second, there is no apparent dependence of the

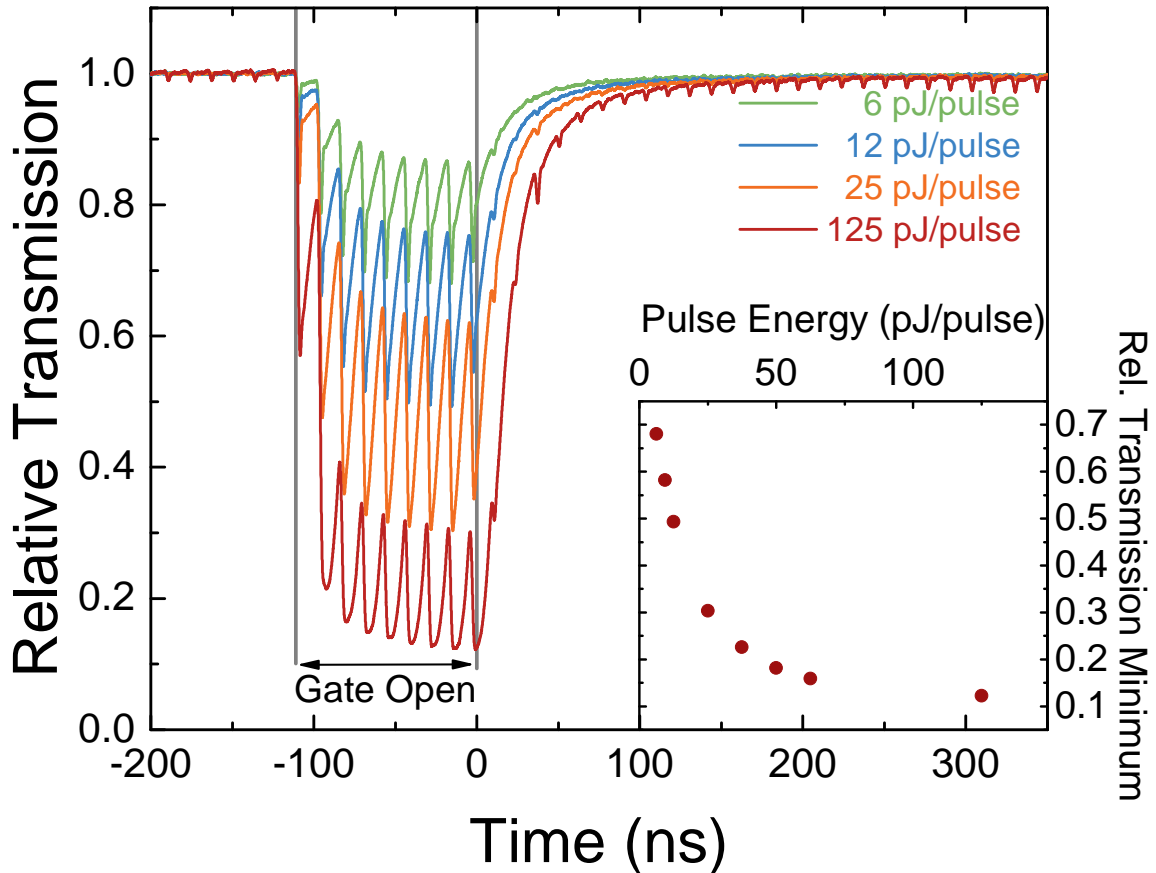


FIG. 3. The relative transmission intensity resolved in time after the arrival of a train of 8 pulses for different pumping energies. The dashed lines represent the temporal region where the gate is open and the system is excited non-resonantly with a pulse repetition rate of $\nu = 75$ MHz. The periodic signal at large pump energies arises due to the finite extinction ratio of about 1:100 of the intensity modulator. Inset: Circles represent the minimum value of the relative transmission for different pumping energies.

relaxation timescale on the non-resonant pump intensity, which suggests that spin-forbidden dark excitons at low momentum form the majority of long-lived carriers. Additionally, we also found a compelling evidence that the interaction between them and bright polaritons is repulsive [14].

In summary, we have demonstrated that a narrow polariton mode may be utilized as a sensitive probe for the presence of dark excitations in a semiconductor system. We found that these carriers have a surprisingly long lifetime of more than 20 ns. Besides the possibility to unveil the dynamics of optically dark excitations, which are difficult to address otherwise, our

result has several important implications. First, it demonstrates the possibility to optically imprint potential landscapes for polaritons that last three orders of magnitude longer than the polariton lifetime in the system. This provides interesting perspectives for functional polariton circuits and classical polariton simulators [25–28]. Resonant injection of dark excitons via two photon absorption [23, 29, 30] might provide means to create tailored optical potentials without perturbing relaxation dynamics. Finally, typical pulsed excitation experiments on polariton systems employ lasers with a pulse separation of about 13 ns. The existence of dark excitations with a lifetime longer than that implies that the standard assumption that the system is completely empty before an excitation pulse arrives is not tenable, which is of high importance for studies of condensate formation.

a. Acknowledgements. We gratefully acknowledge support from the DFG in the framework of TRR 160 within project B7. AK acknowledges the financial support of the Ministry of Education and Science of the Russian Federation in the framework of Megagrant No. 14.Y26.31.0027. CS acknowledges support from the DFG in the framework of project 1376 3-1.

-
- [1] E. Malic, M. Selig, M. Feierabend, S. Brem, D. Christiansen, F. Wendler, A. Knorr, and G. Berghäuser, *Phys. Rev. Materials* **2**, 014002 (2018).
 - [2] S. Bode, C. C. Quentmeier, P.-N. Liao, N. Hafi, T. Barros, L. Wilk, F. Bittner, and P. J. Walla, *Proceedings of the National Academy of Sciences* **106**, 12311 (2009).
 - [3] M. Nirmal, D. J. Norris, M. Kuno, M. G. Bawendi, A. L. Efros, and M. Rosen, *Phys. Rev. Lett.* **75**, 3728 (1995).
 - [4] A. L. Efros, M. Rosen, M. Kuno, M. Nirmal, D. J. Norris, and M. Bawendi, *Phys. Rev. B* **54**, 4843 (1996).
 - [5] H. Kurtze, D. R. Yakovlev, D. Reuter, A. D. Wieck, and M. Bayer, *Phys. Rev. B* **85**, 195303 (2012).
 - [6] I. Schwartz, D. Cogan, E. R. Schmidgall, Y. Don, L. Gantz, O. Kenneth, N. H. Lindner, and D. Gershoni, *Science* (2016), 10.1126/science.aah4758.
 - [7] D. Bajoni, E. Semenova, A. Lemaître, S. Bouchoule, E. Wertz, P. Senellart, S. Barbay, R. Kuszelewicz, and J. Bloch, *Phys. Rev. Lett.* **101**, 266402 (2008).

- [8] M. Amthor, T. C. H. Liew, C. Metzger, S. Brodbeck, L. Worschech, M. Kamp, I. A. Shelykh, A. V. Kavokin, C. Schneider, and S. Höfling, *Phys. Rev. B* **91**, 081404 (2015).
- [9] A. Baas, J. P. Karr, H. Eleuch, and E. Giacobino, *Phys. Rev. A* **69**, 023809 (2004).
- [10] M. Vladimirova, S. Cronenberger, D. Scalbert, K. V. Kavokin, A. Miard, A. Lemaître, J. Bloch, D. Solnyshkov, G. Malpuech, and A. V. Kavokin, *Phys. Rev. B* **82**, 075301 (2010).
- [11] C. Ouellet-Plamondon, G. Sallen, F. Morier-Genoud, D. Y. Oberli, M. T. Portella-Oberli, and B. Deveaud, *Phys. Rev. B* **95**, 085302 (2017).
- [12] M. Wouters, T. K. Paraiso, Y. Léger, R. Cerna, F. Morier-Genoud, M. T. Portella-Oberli, and B. Deveaud-Plédran, *Phys. Rev. B* **87**, 045303 (2013).
- [13] J. Schmutzler, T. Kazimierczuk, O. Bayraktar, M. Aßmann, M. Bayer, S. Brodbeck, M. Kamp, C. Schneider, and S. Höfling, *Phys. Rev. B* **89**, 115119 (2014).
- [14] See Supplemental Material for a full discussion of the estimation of the lifetime of dark excitons, the transition towards weak coupling and the sign of the interaction between polaritons and dark excitations.
- [15] H. Deng, H. Haug, and Y. Yamamoto, *Rev. Mod. Phys.* **82**, 1489 (2010).
- [16] B. Deveaud, F. Clérot, N. Roy, K. Satzke, B. Sermage, and D. S. Katzer, *Phys. Rev. Lett.* **67**, 2355 (1991).
- [17] M. Wouters and I. Carusotto, *Phys. Rev. B* **75**, 075332 (2007).
- [18] S. S. Gavrilov, *Phys. Rev. B* **90**, 205303 (2014).
- [19] The interaction constants are $g_C = 0.45 \mu\text{eV}$ and $g_X = 2g_C$. The relaxation rate is $\gamma_C = 0.17 \text{ps}^{-1}$. The polariton energy detuning is $\delta_p = 180 \mu\text{eV}$. Pulse repetition rate in the Gate is $\nu^{-1} = 13.3 \text{ns}$, duration of one pulse is $w = 200 \text{fs}$. The resonant pump amplitude f and the peak non-resonant pump power P_0 are the fitting parameters.
- [20] J. O. Tollerud, S. T. Cundiff, and J. A. Davis, *Phys. Rev. Lett.* **117**, 097401 (2016).
- [21] D. W. Snoke, W. W. Rühle, K. Köhler, and K. Ploog, *Phys. Rev. B* **55**, 13789 (1997).
- [22] L. Viña, *Journal of Physics: Condensed Matter* **11**, 5929 (1999).
- [23] C. Gautham, M. Steger, D. Snoke, K. West, and L. Pfeiffer, *Optica* **4**, 118 (2017).
- [24] I. Shelykh, L. Viña, A. Kavokin, N. Galkin, G. Malpuech, and R. André, *Solid State Communications* **135**, 1 (2005).
- [25] N. G. Berloff, M. Silva, K. Kalinin, A. Askitopoulos, J. D. Töpfer, P. Cilibrizzi, W. Langbein, and P. G. Lagoudakis, *Nature Materials* **16**, 1120 (2017).

- [26] G. Tosi, G. Christmann, N. G. Berloff, P. Tsotsis, T. Gao, Z. Hatzopoulos, P. G. Savvidis, and J. J. Baumberg, *Nature Physics* **8**, 190 (2012).
- [27] M. Aßmann, F. Veit, M. Bayer, A. Löffler, S. Höfling, M. Kamp, and A. Forchel, *Phys. Rev. B* **85**, 155320 (2012).
- [28] J. Schmutzler, P. Lewandowski, M. Aßmann, D. Niemietz, S. Schumacher, M. Kamp, C. Schneider, S. Höfling, and M. Bayer, *Phys. Rev. B* **91**, 195308 (2015).
- [29] G. Leménager, F. Pisanello, J. Bloch, A. Kavokin, A. Amo, A. Lemaitre, E. Galopin, I. Sagnes, M. D. Vittorio, E. Giacobino, and A. Bramati, *Opt. Lett.* **39**, 307 (2014).
- [30] J. Schmutzler, M. Aßmann, T. Czerniuk, M. Kamp, C. Schneider, S. Höfling, and M. Bayer, *Phys. Rev. B* **90**, 075103 (2014).

Supplementary material: Tracking Dark Excitons with Exciton-Polaritons

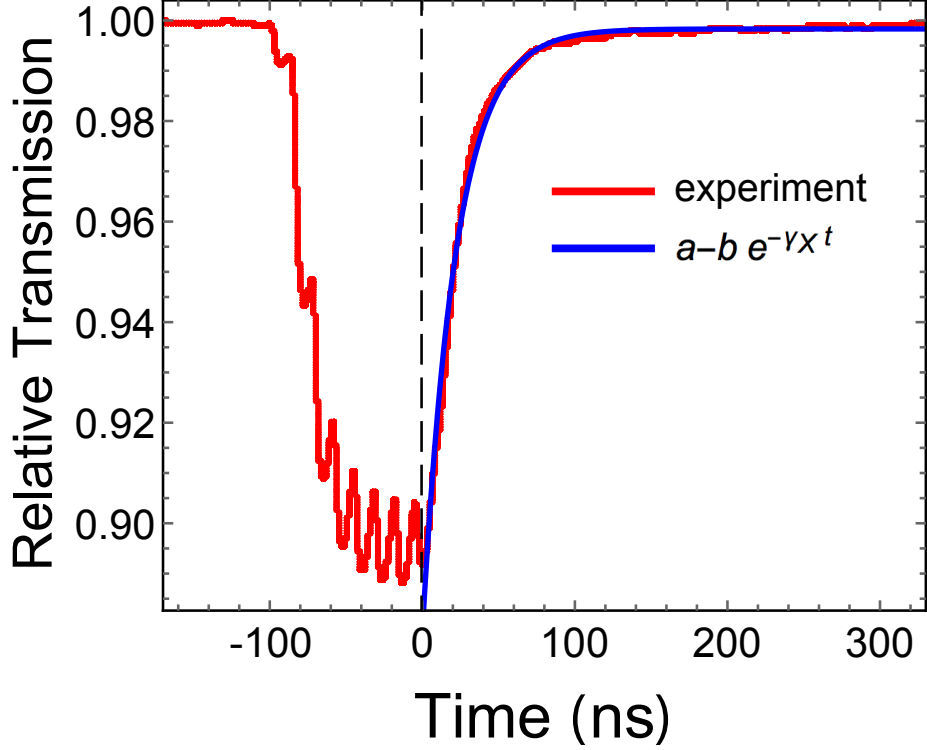


FIG. S1. Relative transmission in time. Red curve corresponds to the experiment. Blue curve shows fitting of the transmission after the last pulse, $t > 0$. The fitting parameters are $a \approx 0.998$, $b \approx 0.12$ and $\gamma_X \approx 45.16 \mu\text{s}^{-1}$.

I. ESTIMATION OF THE LIFETIME OF DARK EXCITONS

Figure S1 and Fig. 2 in the main text show the measured relative transmission variation in time. The dependence consists of three regions: before the gate opens (before ≈ -100 ps), while the gate is open (from -100 to 0 ps) and after the gate closes (after 0 ps). The third region allows one to estimate the lifetime of dark excitons forming the gate.

Since the duration of each pulse in the train (less than 200 fs) is significantly shorter than other characteristic time scales in the system including lifetimes of polaritons and especially dark excitons, one can assume that each non-resonant pulse instantaneously pumps the reservoir of dark excitons, followed by its slow relaxation until the subsequent pulse arrival.

After the last pulse of the train enters the cavity, the occupation number of the dark exciton reservoir starts to decrease monotonically until the end of the system evolution. Rate equation (2) in the main text has a simple solution in this region:

$$N_X = N_{X0}e^{-\gamma_X t} \quad \text{for } t > 0, \quad (\text{S1})$$

where $N_{X0} = N_X(t = 0)$.

Using the fact that the polariton lifetime is much (at least three orders) shorter than that of dark excitons, we can assume the occupancy of the polariton state as well as the transmission through the structure adiabatically adjust to the variation of the occupancy of the dark exciton reservoir. We fit the relative transmission T for $t > 0$ by the function $a - b \exp[-\gamma_X t]$, see Fig. S1. The best matching has been achieved for the fitting parameters $a \approx 0.998$ and $b \approx 0.12$, that allowed us to estimate the relaxation rate and lifetime of dark excitons as $\gamma_X \approx 45.16 \mu\text{s}^{-1}$ and $\tau_X = 1/\gamma_X \approx 22.15 \text{ ns}$, respectively.

II. STRONG-COUPLING TO WEAK-COUPLING TRANSITION

When exciting the microcavity sample above the band gap energy, non-resonantly excited carriers may form polaritons and relax towards the lower polariton branch ground state. Whether this process results in spontaneous exciton-polariton condensation depends strongly on the investigated sample.

Our sample contains six quantum wells and power dependent measurements with non-resonant excitation show no sign of exciton-polariton condensation as is typical for this sample design. However, with increasing non-resonant excitation powers, we observe a transition from the strong-coupling into the weak-coupling regime. This transition can be identified by additional photoluminescence (PL) at energies above the polariton dispersion, where the PL of the bare cavity mode becomes visible (see Fig. S2). For a more quantitative analysis of the transition from the strong-coupling into the weak-coupling regime, we performed a full set of power dependent measurements. Here, we integrated the PL close to $k_{\parallel} = 0$ for energies around the bare cavity mode. The result as well as the area of integration can be seen in figure S3. A clear non-linear increase of the integrated intensity from the bare cavity becomes visible at approximately 350 pJ per pulse. This energy per pulse marks the transition point, where the system leaves the strong-coupling regime and therefore loses

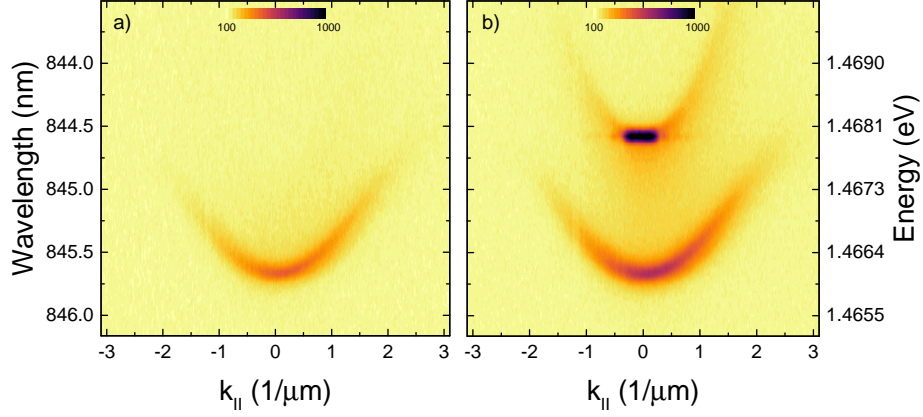


FIG. S2. Far-field image of the lower polariton branch dispersion for two different non-resonant excitation energies per pulse E_{NR} . a) For $E_{NR} = 175$ pJ per pulse, the system is still in the strong-coupling regime, indicated by PL originating solely from the strongly coupled exciton-polariton states. b) For $P_{NR} = 412.5$ pJ per pulse, the system is already in the weak-coupling regime, indicated by the additional PL from the cavity mode.

its polariton eigenstates.

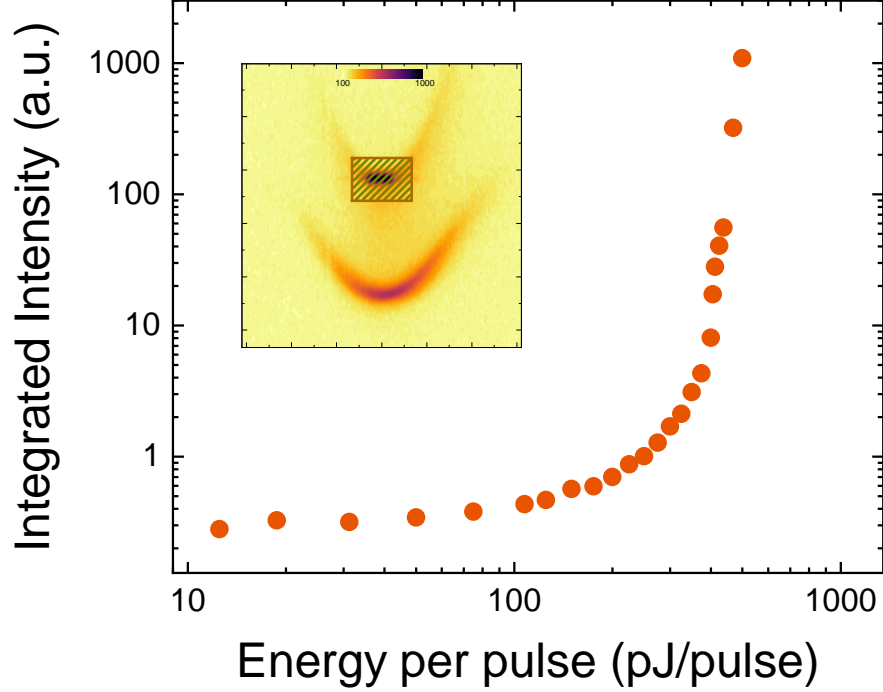


FIG. S3. Time-integrated output from the bare cavity mode under non-resonant excitation using a train of 8 pulses with repetition rate of $\nu_{\text{pick}} = 100$ kHz. The vertical axis is the integrated intensity obtained from the brown dashed box in the inset for various energies per pulse.

III. BLUESHIFT OF POLARITONS

To show that the interaction between the long-lived dark carriers and polaritons is repulsive, we performed time-resolved measurements of the relative transmission for various cw probe beam powers. The powers were chosen such that different significant points along the hysteresis curve are covered (see full dots in the inset of Fig. S4). Then, a train of 7 non-resonant pulses is applied to the sample. Interestingly, when the power of the cw probe beam is below the bistable region (green ball in the inset of Fig. S4), the response of the system is an overall enhancement of the transmission with an additional more significant enhancement after the end of the pulse train. For these cw probe powers the repulsive nature of the dark carriers quickly blueshifts the polariton dispersion towards and beyond the energy of the cw beam. After the last pulse of the train has arrived, the dark excitons slowly start to decay again and the polariton mode is shifted towards lower energies. At some point in time, the polariton dispersion becomes resonant with the pump beam again and as energy of the polariton mode changes much slower during the decay of the reservoir

as compared to its build-up, the enhancement of the transmitted intensity lasts longer and is more pronounced compared to the initial increase. For all cw pump powers within the bistable region, the transmitted intensity is only reduced. This behavior rules out net attractive interactions between dark excitons and polaritons and also other influences such as sample heating, which would result in a redshift of the polariton mode.

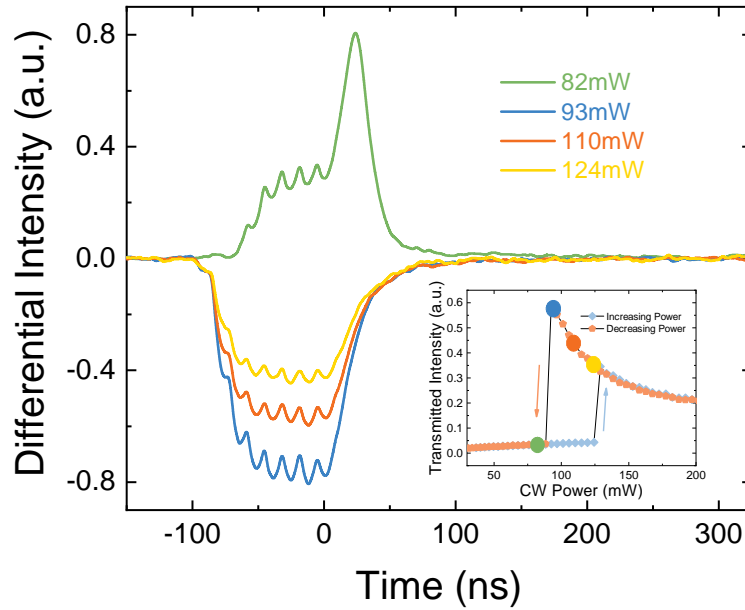


FIG. S4. Time-resolved transmission measurements for different cw pump powers along the hysteresis curve. The vertical axis shows the differential intensity to create a base line of the intensity for every measurement. Inset: Transmitted intensity of hysteresis curve. The different filled dots in in the inset correspond to the cw pump powers chosen for the measurements in the main figure.